A new aberration correction method for photoemission electron microscopy by means of moving focus

2005 J. Phys.: Condens. Matter 17 S1371

(http://iopscience.iop.org/0953-8984/17/16/008)

INSTITUTE OF PHYSICS PUBLISHING JOURNAL OF PHYSICS: CONDENSED MATTER

J. Phys.: Condens. Matter **17** (2005) S1371–S1380 doi:10.1088/0953-8984/17/16/008

A new aberration correction method for photoemission electron microscopy by means of moving focus

T Koshikawa[1,4], **H Shimizu**[1], **R Amakawa**[1], **T Ikuta**[2], **T Yasue**[1] **and E Bauer**[3]

[1] Fundamental Electronics Research Institute and Academic Frontier Promotion Center, Osaka Electro-Communication University, 18-8 Hatsu-cho, Neyagawa, Osaka 572-8530, Japan
[2] Department of Lightwave Sciences, Osaka Electro-Communication University, 18-8 Hatsu-cho, Neyagawa, Osaka 572-8530, Japan
[3] Department of Physics and Astronomy, Arizona State University, Tempe, AZ 85287-1504, USA

E-mail: kosikawa@isc.osakac.ac.jp

Received 9 December 2004
Published 8 April 2005
Online at stacks.iop.org/JPhysCM/17/S1371

Abstract
A new aberration correction method has been developed for photoemission electron microscopy (PEEM). In order to correct the spherical and chromatic aberrations, a moving focus method was adopted. Several experimental limitations to achieving optimal resolution have also been overcome. A high brightness Hg lamp system has been developed to overcome the insufficient brightness of the conventional Hg lamp. An improvement of brightness by over 100 times as compared with the conventional lamp was achieved. Image blur was also found due to a weak environmental AC magnetic field caused by essential microscope components, i.e., the power transformer and CCD camera. After implementing the high brightness lamp and eliminating stray magnetic field by proper shielding, preliminary experiments demonstrate that aberration correction by moving focus can improve the PEEM image resolution.

1. Introduction

Photoemission electron microscopy (PEEM) and low energy electron microscopy (LEEM) are very powerful tools for investigating surface dynamic processes such as crystal growth, catalysis, phase transitions, and so on. The lateral resolutions of PEEM and LEEM are limited by the spherical and chromatic aberrations of the objective lens. Because there is no concave lens in the electron optics, it is impossible to eliminate aberrations by the combination of concave and convex lenses. Great efforts have been made to correct aberrations from the very

[4] Author to whom any correspondence should be addressed.

beginning of the development of the electron microscope, but these efforts have not paid off. As for PEEM, a few methods to correct aberrations have been proposed. One method is to use an electron mirror corrector. The principle of aberration correction by the electron mirror was originally proposed by Scherzer [1], and a practical application to the emission microscope was discussed by Rose and Preikszas [2]. A tetrode mirror corrector [3] has been adopted in the SMART project [4–6] to compensate spherical and chromatic aberrations simultaneously. Developmental work on the SMART project has been carried out since 1997. Another approach to correcting spherical and chromatic aberrations was taken by Schönhense and Spiecker [7]. They used a time-of-flight technique to realize aberration correction. Correction of the chromatic aberration was practically achieved, but correction of the spherical aberration might be quite difficult technically.

In the present study, we developed a new aberration correction method for PEEM by using a moving focus method [8]. The basic concept of the spherical aberration correction and the reduction of the influence of the chromatic aberration using a moving focus method is described in the next section. During the development of the new aberration correction method for PEEM, we faced several technical problems which had to be resolved. Solutions of these problems will be described in section 3. Finally, we show the preliminary results on the aberration correction to demonstrate the validity of the moving focus method. These results were obtained using a new high brightness Hg lamp in the laboratory. Application of the moving focus method will also be made in experiments that will be carried out at a synchrotron radiation (SR) facility in the future.

2. Aberration correction by a moving focus method

The basic idea of aberration correction by the moving focus method was proposed by Ikuta in 1985 [8]. In incoherent imaging, it has been shown by Häusler that the depth of focus can be increased by image during the moving focus [9]. This is illustrated in figure 1(a). We consider two optical paths through the objective lens. Figure 1(a) shows the interference of two plane waves with the same angles to the optical axis. The interference fringes form parallel to the optical axis. When the intensities of the interference fringes along the optical axis are integrated during moving focus, the interference fringes remain. This indicates the increase of the depth of focus. However, the object transfer function (OTF) after integration shows strong damping in the high spatial frequency region. In order to recover the damping, a Häusler-type filter is effective [9]. It has been shown by Ikuta that the moving focus does not merely increase the depth of focus but also eliminates the influence of the spherical aberrations [8].

In order to understand the principle of aberration correction by moving focus, consider two plane waves that have different angles with respect to the optical axis. Figure 1(b) shows the optical paths of two such plane waves. In this case, the interference fringes are not parallel to the optical axis. That is, the interference between optical paths with different angles through the objective lens contributes to a uniform background in the image superposition produced by moving focus. Therefore, moving focus eliminates the contribution of interference of all plane waves except those that have the same angle with the optical axis. In this case, the optical path lengths of the two waves in the surviving pairs are identical, so that the influence of the spherical aberration is eliminated. This means that the correction of the spherical aberration would be possible using the moving focus method.

Next, we consider the influence of the chromatic aberration of the objective lens. Due to the chromatic aberration, the focal point spreads along the optical axis for waves with different wavelengths. This means that the chromatic aberration has nearly the same effect on the image on the focal point as the moving focus.

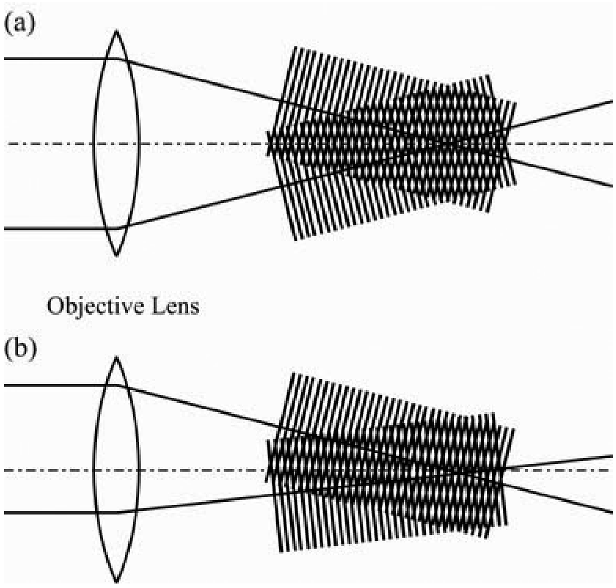

Figure 1. The principle of the aberration correction by the moving focus method. (a) The interference of two plane waves with the same angle to the optical axis, (b) that of plane waves with different angles. The interference fringes form parallel to the optical axis in (a), while they incline to the optical axis in (b).

An important point to consider in the application of the moving focus method is the range of moving focus. The range of moving focus is determined by the contrast aperture diameter and spherical aberration coefficient. Electron waves passing through the different points on the objective lens have different focal lengths and therefore cross the optical axis at different points relative to the contrast aperture plane. The range of moving focus is determined by this spread of focal positions. Definitely, moving focus would cover the distance between the focal points for the paraxial wave and for the outermost wave within the contrast aperture, which is a function of the spherical aberration coefficient.

The influence of the spherical aberration should be corrected by the moving focus method, and the chromatic aberration could be partially reduced. Then the resolution would be determined by several factors, such as diffraction limit, environmental influence, stability of the apparatus, and so on. Aberration correction of PEEM based on core electrons with well defined energies using the energy filter would be expected to improve resolution to below 10 nm.

Figure 2 demonstrates the fundamental results of the aberration correction with the moving focus method which was carried out using an optical microscope. An optical objective lens with numerical aperture of 0.6 was used, and the wavelength of light was 0.65 μm. Figure 2(a) shows the original dark field image including the spherical aberration of dust particles. Since the particle has a three-dimensional structure, a part of the particle is focused, but the other part of the particle is not so clear. Figure 2(b) shows the aberration-corrected image after applying the moving focus method by varying the sample stage position. As is clearly seen, the lateral resolution is somewhat improved and the depth of focus is increased.

The moving focus method has been applied to transmission electron microscopy (TEM) by Shimizu's project [10, 11]. A series of defocus images was obtained by modulating the acceleration voltage, and they were integrated after weighting with the contrast transfer

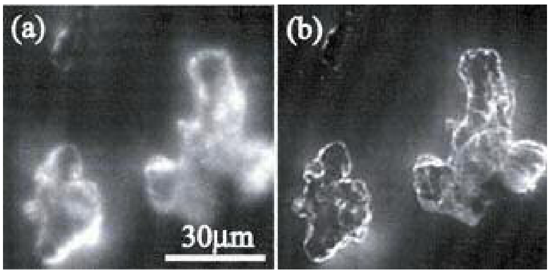

Figure 2. Results on the fundamental aberration correction experiments using the optical microscope. (a) The original image of dust particles including spherical aberration. (b) The aberration-corrected image using the moving focus method.

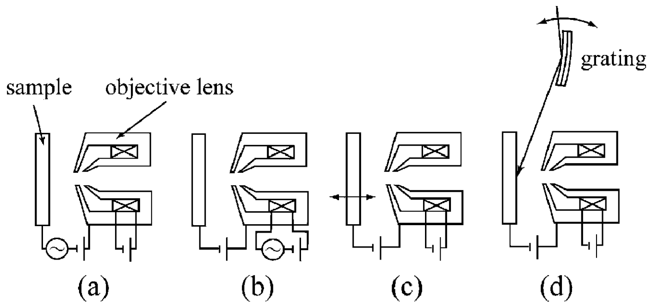

Figure 3. Practical moving focus ways applicable to PEEM. (a) Moving electric field between the sample and the objective lens, (b) moving magnetic field of the objective lens, (c) moving sample position and (d) moving wavelength of the incident light.

function. In conventional TEM images, extra lattice fringes due to the spherical aberration appear outside the crystal even at the Scherzer focus. After applying the moving focus method, they showed a clear atomic image without the extra fringes. This serves to establish the viability of the moving focus method in electron microscopy. The imaging mechanism of PEEM, however, is quite different from that of TEM. In TEM, the coherent diffracted electrons are imaged, whereas PEEM images with incoherent photo-emitted electrons. The implication is that moving focus methods have to be considered for PEEM that are different from those that are applied to TEM. Figure 3 shows the several practical moving focus methods applicable to PEEM. Figures 3(a) and (b) show the modulation of the electric or magnetic field of the objective lens, respectively. The applied voltage between the sample and the first electrode of the objective lens is modulated in the former case, and the electric current exciting the magnetic objective lens is modulated in the later case. In the present study, we have adopted the method of modulating the magnetic field. Figure 3(c) shows the moving focus by modulation of the sample position. A high voltage of 20 kV is applied to the sample in our PEEM system, which makes it difficult to manipulate the sample position with sufficient precision to realize the moving sample position method. Figure 3(d) shows the moving wavelength of the incident photon beam. The moving wavelength might be effective at a synchrotron facility.

Figure 4(a) is a picture of our PEEM system, and a schematic diagram of the newly developed aberration correction system for PEEM is shown in figure 4(b). The basic set-up of our PEEM system is the same as the spectroscopic photoemission and low energy electron microscopy (SPELEEM) [12]. Briefly, the apparatus consists of an electron gun column, a 60° deflected beam separator, a magnetic objective lens, an imaging column, a hemispherical

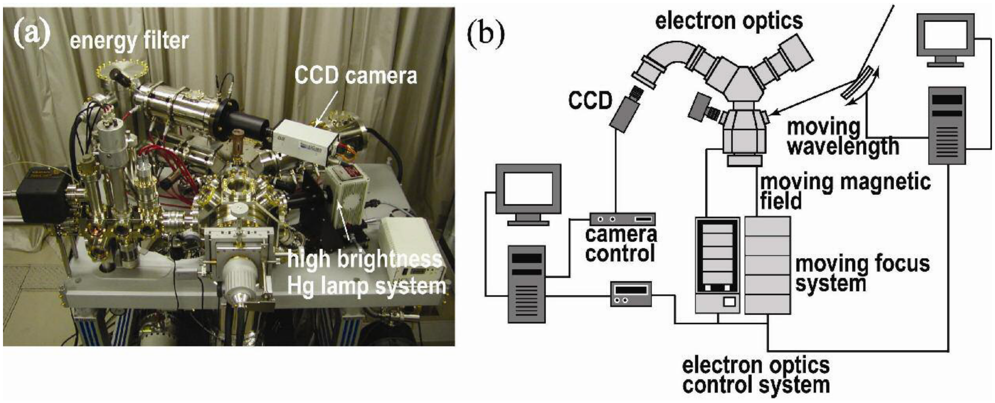

Figure 4. (a) A picture of the aberration corrected PEEM instrument. (b) A schematic diagram of the whole system of the developed aberration-corrected PEEM using the moving focus method.

imaging energy filter and a projection lens system. The three-stage sample preparation chamber is attached. Details of the high brightness Hg lamp system will be given in the next section.

A newly developed aberration correction system for PEEM consists of an electron optics control system, and an image acquisition system including a CCD camera and a moving focus system. In figure 4(b), the moving focus system by the modulation of the magnetic field of the objective lens and that of the wavelength of the SR light is illustrated. For laboratory use, the wavelength moving system is not mounted, and instead a high brightness Hg lamp system, which will be described in the next section, is attached.

The moving focus system generates the modulation signal applied to the objective lens or the monochromator, and also controls the image acquisition system. The image acquisition is synchronized with the moving focus signal. Image processing, such as Fourier transformation, filtering and so on, is carried out on-line just after the end of the image acquisition. The time required for image processing, however, does not limit the image acquisition rate because the computing speed of the conventional personal computer is enough high to do the image processing in almost real time. Then the image acquisition time is mainly limited by the time during which the modulation signal is applied. The response of the magnetic objective lens may limit the repetition rate to several hertz. In the case of the modulation of the wavelength or the electric field shown in figure 3(a), the repetition rate of modulation would be increased. The other factor in determining the acquisition rate is the brightness of the light source. For secondary electron imaging excited by intense SR light near an absorption edge, the acquisition time would be short. On the other hand, long exposure will be required in the case of imaging based on electrons generated by core excitation.

3. Problems in fundamental experiments and their improvements

3.1. Brightness of Hg lamp

In order to detect the improvement of the lateral resolution of PEEM by aberration correction, a highly magnified image is required. An Hg lamp was used as a light source in the present fundamental experiment. The brightness of the conventional Hg lamp, however, is not sufficient to observe the highly magnified PEEM image. In order to overcome this problem, we developed a new high brightness Hg lamp system for laboratory use in collaboration with ULVAC-PHI

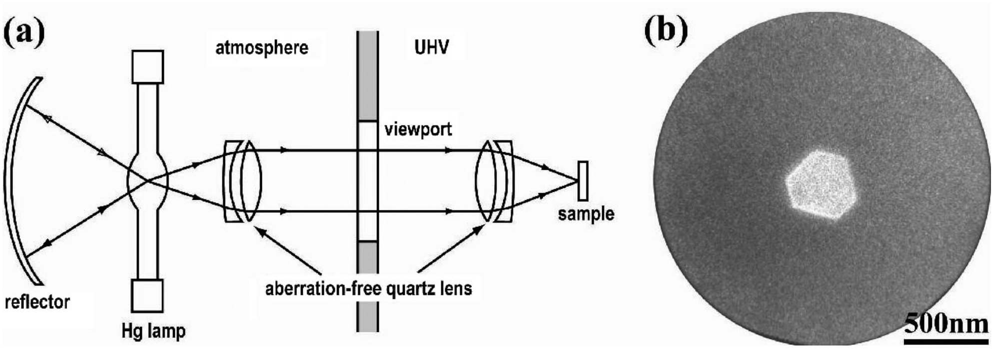

Figure 5. (a) Schema of a newly developed high brightness Hg lamp system. (b) PEEM image of a three-dimensional Pb crystal on a W(110) surface using the high brightness Hg lamp system. The field-of-view is 2 μm.

Inc. Figure 5(a) shows a schematic diagram of the high brightness Hg lamp system. The lamp used is a commercial 100 W Hg lamp, whose effective arc size is 0.25×0.25 mm^2. A pair of identical aberration-free quartz lens systems were newly designed and placed in between the Hg lamp and the sample. One lens system is in atmosphere and the other is in the vacuum chamber. The Hg lamp and the sample are placed in the focal planes of the lens system. The magnification of the new Hg lamp system is unity. A parallel light beam is obtained between the two lens systems in this arrangement, so that a quartz viewport for UHV can be used without any disturbance to the optical property of the entire system except for absorption. An improvement of brightness by a factor of 126 relative to the conventional Hg lamp is expected based on ray tracing. Figure 5(b) shows the PEEM image of a three-dimensional Pb crystal on a W(110) surface that was obtained using the newly developed Hg lamp system. The field-of-view is 2 μm, and the image exposure time is 10 s. Based on this image obtained with the high brightness Hg lamp system, we estimate that an improvement of brightness of more than 100 times has been realized experimentally compared to the conventional Hg lamp.

3.2. *Environmental magnetic AC field*

The highly magnified LEEM images and PEEM images that were made possible by the high brightness Hg lamp system revealed other problems that were related to environmental influences. Figure 6(a) shows an LEEM image of Pb on a Si(111) surface. The field-of-view is 2 μm. Note that the dark spots seen in the image are defects of the microchannel plate detector screen. The bright intensity regions in the image indicate the decoration of steps and domain boundaries of the Si(111) surface by Pb. However, the contrast is not sufficiently sharp to observe the details. There are several plausible origins of such blur of the image. We carefully checked the influence of astigmatism, instability of the power supply, vibrations, and so on, but ruled out these explanations. It was discovered that a weak environmental AC magnetic field generated by the power transformer and CCD camera was the origin of the blur of the image. The pictures are shown in the inset of figure 6(a). The strength of the magnetic field at the sample chamber was about 1.23 mG rms. This field was reduced to about 0.23 mG by shielding the transformer and the CCD camera by steel whose thickness is 3 mm, as shown in inset of figure 6(b). The LEEM image after shielding is shown in figure 6(b). The blur of the image is noticeably less than that in figure 6(a), and sharp bright features can be seen.

Since the magnetic field around the sample and the objective lens is shielded by Permalloy in the UHV chamber, the environmental weak magnetic field probably affects the electron

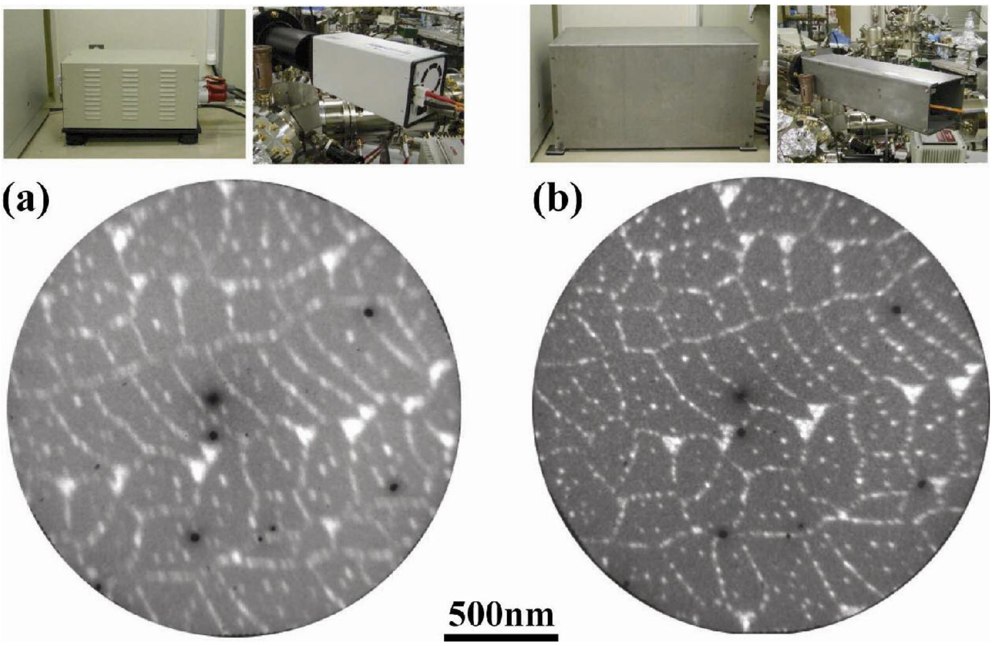

Figure 6. Influence of the environmental weak magnetic AC field. (a) LEEM image of Pb/Si(111) with the stray magnetic field. (b) LEEM image with the stray magnetic field shielding. The field-of-view is 2 μm. The inset shows pictures of the transformer and CCD camera which are the source of the stray magnetic field before and after shielding by the steel box.

beam in other parts of the instrument, for example, the beam separator or imaging column, even though electrons pass through them with 20 keV kinetic energy. The CCD camera is placed particularly close to the beam separator in our system as shown in figure 4(a), so that careful shielding of the weak magnetic field from the CCD camera is quite important. At present the transformer and the CCD camera are shielded by double Permalloy boxes. The strength of the stray magnetic field is less than one fifth of that with the steel box.

4. Results of preliminary aberration correction experiments

The preliminary experiments of the aberration correction were carried out by using the newly developed high brightness Hg lamp system. Figure 7(a) shows a diagram of the aberration correction experiments. The moving focus signal is applied to the magnetic objective lens, and the image acquisition by the CCD camera is synchronized to the modulation signal. Then a series of moving focus images is accumulated within the exposure of the CCD. But the moving focus was carried out stepwise and the moving focus images were simply added up in the present preliminary experiments. In the obtained accumulated image with moving focus, however, the high spatial frequency components are reduced in principle as described above. Then the Häusler high frequency enhancement filter is applied in the Fourier space in order to recover the whole information included in the accumulated image. Finally the aberration corrected image can be obtained by applying the inverse Fourier transformation.

Figure 7(b) shows the conventional PEEM image of the Pb/Si(111) surface. The field-of-view is 4 μm. A bright contrast can be seen along the step edges and the domain boundaries. Fine structures, however, are not so clear because of the poor lateral resolution. Then the

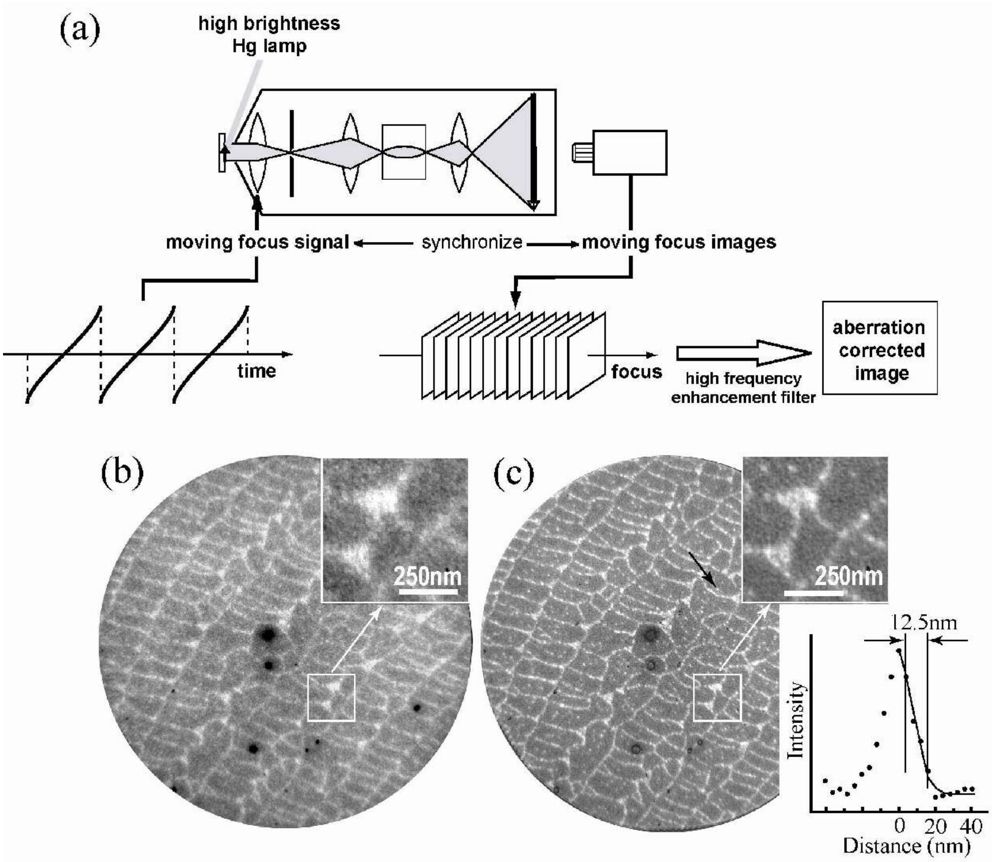

Figure 7. The preliminary results of the aberration correction using the high brightness Hg lamp system in the laboratory. (a) A schematic diagram of the experiment, (b) the conventional PEEM image and (c) the aberration-corrected PEEM image using the moving focus method. The sample is Pb/Si(111) and the field-of-view is 4 μm.

new aberration correction method is applied. As mentioned before, the range of moving focus depends on the spherical aberration coefficient after acceleration in the electric field between the sample and the objective lens. The precise relationship between the spherical aberration after acceleration and that on the sample, however, is not clear up to now. Furthermore, the relationship between the amount of moving focus on the sample and the objective lens current is also not clear. We examined several ranges of moving focus by changing the objective lens current. We found that the image becomes clearer when the range of moving focus was increased, and almost saturates in its quality at a certain range of objective lens current. The superposition of 41 successive images obtained without the contrast aperture during the moving focus was carried out without any weighting. The exposure time of each image was 10 s. In the present preliminary experiments, we changed the objective lens current by 0.02 mA steps. The step is determined to get a sufficient signal-to-noise ratio of the aberration-corrected PEEM image in the present experimental conditions. The Häusler-type high frequency enhancement filter should be applied to recover the degradation of the OTF of the superimposed image. In the present experiments, however, the precise OTF of the present apparatus is not known, so we examined several suitable modified values of the Häusler-type high frequency enhancement filter function. The improved PEEM image is shown in figure 7(c). In order to obtain the improved PEEM image, the high spatial frequency component above about 48 μm^{-1} was weighted by the factor of 10 compared with the low spatial frequency component below about 2.4 μm^{-1}, and the weight was linearly interpolated in between these two spatial frequencies. The high frequency cutoff was set at about 194 μm^{-1}. The fine structures can be well distinguished in the image. The measured edge resolution for an isolated fine structure indicated by a black arrow is about 12.5 nm, as shown in the inset, although the size of each pixel is not sufficiently small to discuss the finer details of the resolution. In addition to the improvement of the resolution, the improved PEEM image seems to be much sharper, since the trailing edge of the cross section of white dots in figure 7(c) is strongly reduced in comparison with that in figure 7(b). The high frequency enhancement filter used here, however, may not be the unique solution, so that further detailed examination would be necessary.

Chromatic aberration is more dominant than spherical aberration for low kinetic energy photoelectrons excited by the Hg lamp, but the importance of chromatic aberration is diminished for SR-based core excitation with the energy filter. In order to emphasize the spherical aberration correction by the moving focus method, experiments using SR light are required. We have already started the preliminary experiments in SPring-8, which is one of the biggest SR facilities in the world, and the details will be reported in the future.

5. Summary

A new aberration correction method for PEEM using the moving focus was developed in the present study. There were several problems to carry out the fundamental experiments on the aberration correction. In order to overcome the insufficient brightness of the conventional Hg lamp, we developed a new high brightness Hg lamp system. This system improved brightness over 100 times as compared with the conventional Hg lamp illumination. Elimination of the weak environmental AC magnetic field from the transformer and the CCD camera was also crucial for improving the highly magnified PEEM image. Magnetic shielding by steel was quite effective in reducing the stray field, and observation of a high quality sharp image was achieved.

Preliminary experiments on the aberration correction using the newly developed high brightness Hg lamp system were carried out, and an improved resolution of about 12.5 nm was achieved. The obtained results demonstrate that the moving focus method can effectively improve the lateral resolution of PEEM. More improved resolution could be expected for SR-based core excitation images.

Acknowledgment

This work was supported by a Grant-in-Aid for Creative Scientific Research (No. 13GS0022) from the Ministry of Education, Culture, Sports, Science and Technology, Japan.

References

[1] Scherzer O 1947 *Optik* **2** 114
[2] Rose H and Preikszas D 1992 *Optik* **92** 31
[3] Preikszas D and Rose H 1997 *J. Electron Microsc.* **1** 1
[4] Fink R, Weiss M R, Umbach E, Preikszas D, Rose H, Spehr R, Hartel P, Engel W, Degenhardt R, Kuhlenbeck H, Wichtendahl R, Erlebach W, Ihmann K, Schlgl R, Freund H-J, Bradshaw A M, Lilienkamp G, Schmidt Th, Bauer E and Benner G 1997 *J. Electron Spectrosc. Relat. Phenom.* **84** 231

[5] Wichtendahl R, Fink R, Kuhlenbeck H, Preikszas D, Rose H, Spehr R, Hartel P, Engel W, Schlögl R, Freund H-J, Bradshaw A M, Lilienkamp G, Schmidt Th, Bauer E, Benner G and Umbach E 1998 *Surf. Rev. Lett.* **5** 1249

[6] Schmidt Th, Groh U, Fink R, Umbach E, Schaff O, Engel W, Richter B, Kuhlenbeck H, Schlögl R, Freund H-J, Bradshaw A M, Preikszas D, Hartel P, Spehr R, Rose H, Lilienkamp G, Bauer E and Benner G 2002 *Surf. Rev. Lett.* **9** 223

[7] Schönhense G and Spiecker H 2002 *J. Vac. Sci. Technol.* B **20** 2526

[8] Ikuta T 1985 *Appl. Opt.* **24** 2097
Ikuta T 1989 *J. Electron Microsc.* **38** 415

[9] Häusler G 1972 *Opt. Commun.* **6** 38

[10] Kimura Y, Takai Y, Kawasaki T, Shimizu R, Ikuta T, Isakozawa S, Satou Y and Ichihashi M 1999 *J. Electron Microsc.* **48** 873

[11] Takai Y, Kimura Y, Ikuta T, Shimizu R, Sato Y, Isakozawa S and Ichihashi M 1999 *J. Electron Microsc.* **48** 879

[12] Schmidt Th, Heun S, Slezak J, Diaz J, Prince K C, Lilienkamp G and Bauer E 1998 *Surf. Rev. Lett.* **5** 1287